

## Wetting by polymers of a liquid–liquid interface: Effects of short-range interactions and of chain stiffness

Marcel C. P. van Eijk and Frans A. M. Leermakers

Citation: *J. Chem. Phys.* **110**, 6491 (1999); doi: 10.1063/1.478552

View online: <http://dx.doi.org/10.1063/1.478552>

View Table of Contents: <http://jcp.aip.org/resource/1/JCPSA6/v110/i13>

Published by the [American Institute of Physics](#).

---

### Additional information on *J. Chem. Phys.*

Journal Homepage: <http://jcp.aip.org/>

Journal Information: [http://jcp.aip.org/about/about\\_the\\_journal](http://jcp.aip.org/about/about_the_journal)

Top downloads: [http://jcp.aip.org/features/most\\_downloaded](http://jcp.aip.org/features/most_downloaded)

Information for Authors: <http://jcp.aip.org/authors>

### ADVERTISEMENT

**AIP**Advances

*Submit Now*

### Explore AIP's new open-access journal

- Article-level metrics now available
- Join the conversation! Rate & comment on articles

# Wetting by polymers of a liquid–liquid interface: Effects of short-range interactions and of chain stiffness

Marcel C. P. van Eijk<sup>a)</sup> and Frans A. M. Leermakers

Laboratory for Physical Chemistry and Colloid Science, Wageningen Agricultural University, Dreijenplein 6, 6703 HB Wageningen, The Netherlands

(Received 19 May 1998; accepted 5 January 1999)

The behavior of both flexible and semiflexible polymers near a liquid–liquid interface is investigated with the aid of the self-consistent-field theory as developed by Scheutjens and Fler. A ternary system ( $A/B_N/C$ ) is studied near the wetting transition. In a symmetric system, i.e.,  $\chi_{AB} = \chi_{BC} = \chi$ , a change in the interaction parameter  $\chi$  introduces a wetting transition. The ratio of the interfacial width  $\xi$  of the binary  $A/C$  system and the coil size of the polymer determines the order of this transition. Beyond a certain chain length  $N_c$  (at fixed  $\xi$ ) the wetting transition is of first order, whereas it is of second order for  $N < N_c$ . The characteristics of the prewetting line, including the prewetting critical point, are discussed in some detail. The nontrivial  $N$ -dependence of the position of this critical point is analyzed in terms of a crude thermodynamic model. For a semiflexible polymer an increase of the chain stiffness at a certain value of  $\chi$  is sufficient to introduce a wetting transition. © 1999 American Institute of Physics. [S0021-9606(99)70213-8]

## I. INTRODUCTION

In a preceding paper<sup>1</sup> we have discussed the adsorption of a semiflexible polymer at a liquid–liquid interface. There, we restricted ourselves to a situation where the polymer was soluble in both liquid phases, and we only considered small amounts of polymer in the system (Gibbs layers). However, good solvents for polymers are not common, and most frequently the polymer is only marginally soluble. As a consequence, the amounts of polymer, e.g., in industrially relevant multiphase systems, often exceed the solubility limit in one or both of the constituting phases. It is therefore worthwhile to investigate the behavior of semiflexible polymers in a multiphase system at less ideal conditions. If one adds polymer to a two-phase system of monomeric components, one can expect to arrive at a point where a third, polymer-rich, phase emerges. This phase will preferably appear at the interface between the two liquids.<sup>1</sup> This phenomenon is generally denoted as wetting. Before considering the polymeric system, it is worth while to review some basic features of wetting. We choose to do this from a physical adsorption perspective. We base this introduction on a number of excellent reviews on this subject.<sup>2–4</sup>

### A. Contact angles and surface tension

Consider a small liquid droplet at the interface of two other liquid phases. The droplet will adopt a lens-like shape as depicted in Fig. 1. We distinguish two different equilibrium states: partial wetting with  $\theta_1 + \theta_3 > 0$ , and complete wetting for  $\theta_1 + \theta_3 = 0$ . The contact angles can be fully defined in terms of thermodynamic parameters. The Young equation, originally derived from mechanical arguments for

wetting in the presence of a solid surface, is replaced by a set of three equations for a drop at a liquid–liquid interface:

$$\gamma_{13} = \gamma_{12} \cos \theta_1 + \gamma_{23} \cos \theta_3, \quad (1.1a)$$

$$\gamma_{12} = \gamma_{13} \cos \theta_1 + \gamma_{23} \cos \theta_2, \quad (1.1b)$$

$$\gamma_{23} = \gamma_{12} \cos \theta_2 + \gamma_{13} \cos \theta_3, \quad (1.1c)$$

where  $\gamma_{ij}$  is the interfacial free energy per unit area (or interfacial tension) between phase  $i$  and  $j$ . From this set of equations one easily arrives at explicit expressions for the contact angles as a function of the interfacial free energies:

$$\cos \theta_1 = \frac{\gamma_{12}^2 + \gamma_{13}^2 - \gamma_{23}^2}{2 \gamma_{12} \gamma_{13}}, \quad (1.2a)$$

$$\cos \theta_2 = \frac{\gamma_{12}^2 + \gamma_{23}^2 - \gamma_{13}^2}{2 \gamma_{12} \gamma_{23}}, \quad (1.2b)$$

$$\cos \theta_3 = \frac{\gamma_{13}^2 + \gamma_{23}^2 - \gamma_{12}^2}{2 \gamma_{13} \gamma_{23}}. \quad (1.2c)$$

### B. The wetting transition

In a system of three fluid phases as depicted in Fig. 1 one phase sits between the two others either as a lens-shaped drop (partial wetting) or as a macroscopically thick film (complete wetting). There may exist a certain temperature  $T_w$  at which the system switches from one regime to the other. This is the so-called wetting transition temperature. Similar observations can be made for systems where a solid surface is present. To grasp some basic ideas of wetting we first consider a binary system near a solid wall. Below, however, we will apply these ideas also to a system with a liquid–liquid interface. The system will phase separate below a certain critical temperature  $T_c$ . We denote the chemical potential of a component at the coexistence line by  $\mu_0$ . An

<sup>a)</sup>Current address: Physical Chemistry 1, Chemical Centre, Lund University, P.O. Box 124, 221 00 Lund, Sweden. Electronic mail: marcel.vaneijk@fkem1.lu.se

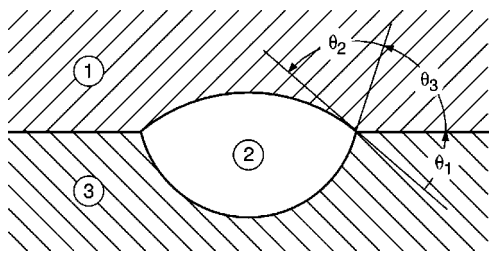


FIG. 1. A three-phase system where phase 2 partially wets the interface between the two other phases. The lens-shaped drop is characterized by the three contact angles as indicated, with  $\theta_1 + \theta_2 + \theta_3 = \pi$ .

appropriate quantity to gain insight into the wetting phenomenon is the excess amount or surface coverage, which in the presence of a solid surface can be defined as

$$\Theta^{\text{exc}}(\mu, T) = \int_0^\infty dz [\rho(z; \mu, T) - \rho(\infty; \mu, T)], \quad (1.3)$$

where the solid surface is located at  $z=0$  and  $\rho$  is the number density of a component.

A first question that arises, is how the excess amount changes with  $\mu$  and  $T$  near various phase boundaries. Furthermore, one wishes to know what would happen if only certain interactions within the system are altered. In Figs. 2(a)–(d) we visualize how  $\Theta^{\text{exc}}(\mu, T)$  may vary along typical cuts in the phase diagram. Comparing Figs. 2(a)–(d) with 2(e)–(h) shows the structural change of  $\Theta^{\text{exc}}(\mu, T)$  which might occur when changing the interaction potentials. Figure 2(a) shows how the coexistence line is approached from the low-density side along two different paths. In both cases  $\Theta^{\text{exc}}$  increases [see Fig. 2(b)]. However,  $\Theta^{\text{exc}}(\mu_0^-, T < T_w)$  remains finite, whereas  $\Theta^{\text{exc}}(\mu_0^-, T \geq T_w)$  diverges for  $\mu \uparrow \mu_0$ . The latter case is usually referred to as complete wetting. The former case is called partial wetting, i.e., a microscopic phase is in equilibrium with a macroscopic phase (droplet). The question now arises how  $\Theta^{\text{exc}}(\mu_0^-, T < T_w)$  develops if the temperature is increased. To this end we consider the paths at  $\mu_0^-$  in Figs. 2(c) and (e). The second-order wetting transition is characterized by a smooth divergence of  $\Theta^{\text{exc}}(\mu_0^-, T)$  for  $T \rightarrow T_w$ , as in Fig. 2(d). The order of the wetting transition depends delicately on the interactions in the system. The wetting transition is of first order if  $\Theta^{\text{exc}}(\mu_0^-, T)$  jumps from a finite value at  $T_w^-$  to a macroscopic value at  $T_w^+$ . This infinite jump at coexistence develops smoothly from finite jumps in the one-phase region [see Figs. 2(e)–(h)]. A finite jump in the one-phase region is usually referred to as prewetting.

### C. Wetting in the presence of polymer chains

In this study we focus on the wetting behavior of flexible and semiflexible polymers in a binary monomeric system within a mean-field approach. We will show that not only the interaction parameters, but also the chain stiffness and chain length have a significant influence on the wetting process. The theoretical approach of this problem is comparable to that applied in our previous paper on adsorption of semiflexible polymer chains at a liquid–liquid interface.<sup>1</sup> In this respect it is also worthwhile to take into consideration the

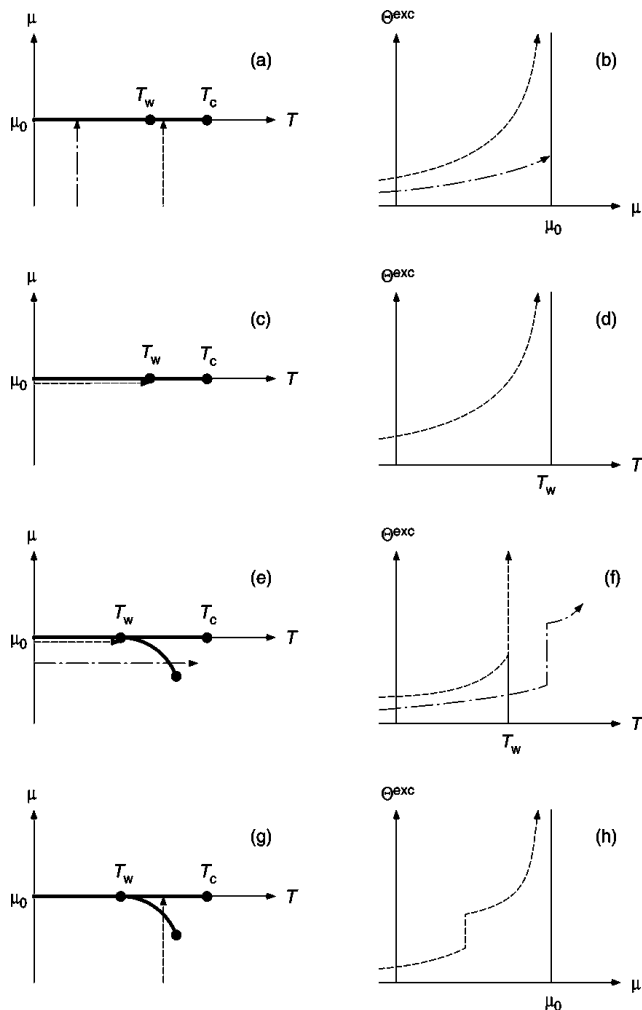


FIG. 2. Excess amount (right panels) along several paths in the bulk phase diagram (left panels) for a binary mixture near a solid wall. The coexistence line ( $\mu = \mu_0, T \leq T_c$ ) separating the two phases is the locus of singularities in the bulk free energy. The interfacial free energy has singularities at  $T_w$  and along the so-called prewetting line sticking out into the one-phase region as in (e) and (g). The difference between (a)–(d) and (e)–(h) lies in this example solely in the interaction with the solid surface.

work carried out on segregation phenomena in polymer blend systems. Mixtures of stiff and flexible chains were studied both by Monte Carlo simulation<sup>5,6</sup> and by a self-consistent-field theory.<sup>7</sup> From these papers we already deduced that the precise nature of the boundary conditions in theoretical studies restricts the number of accessible systems. Other studies into the effects of polymer chain architecture on segregation in polymer blends all point towards a delicate balance between entropic and enthalpic phenomena.<sup>8–11</sup> Because these studies are all restricted to the dilute part of the adsorption isotherm, they can only give hints towards a prediction of the actual wetting behavior in our system. The nature and position of the wetting transition has to be looked at in more detail to gain some understanding. We apply a theory based on a self-consistent-field approximation by Scheutjens and Fleer<sup>12,13</sup> and elaborated by Leermakers and Scheutjens.<sup>14</sup>

## II. THEORY AND METHODS

The self-consistent-field theory of Scheutjens and Fleer (SF SCF) was originally developed to describe the equilib-

rium properties of adsorbing flexible polymer chains at a solid surface. The implementation of the presence of a liquid–liquid interface into this theory is rather straightforward; it simply requires the proper boundary conditions (reflecting at both ends) with a sufficient effective repulsion between the molecular components. The implementation of chain stiffness is more involved and requires a higher-order Markoff formalism for the chain statistics. Leermakers and Scheutjens<sup>14</sup> did the latter for the case of associated colloids. For the present study it is important to note that the nearest-neighbor interactions between segments of type  $x$  and  $y$  are represented by Flory–Huggins interaction parameters  $\chi_{xy}$ , and that a controllable chain stiffness is achieved by the use of third-order Markoff statistics to describe the chain conformation. The latter means that a rotational isomeric state (RIS) model is used, characterized by an energy difference  $\Delta u_{tg}$  between the gauche and the trans state, where the trans state is chosen as the reference state. With this energy difference one is able to calculate the persistence length of the polymer chain<sup>1</sup> as

$$q = b \frac{5\omega + 4}{6\omega} \quad \text{for large } N, \quad (2.1)$$

where  $b$  denotes the bond length,  $N$  the number of bonds, and  $\omega = \exp(-\Delta u_{tg}/k_B T)$ .

The systems under consideration in this study all consist of two monomeric components,  $A$  and  $C$ , and of a homopolymer  $B_N$ . To keep the system characteristics transparent we restrict ourselves to a, from a polymer perspective, symmetric system, i.e.,  $\chi \equiv \chi_{AB} = \chi_{BC}$ .

Before discussing the process of wetting, we first consider the bulk phase diagram. To calculate this diagram, we do not need the SF SCF theory for inhomogeneous systems; it suffices to use the classical Flory–Huggins theory. For the three components we can write the Helmholtz (or free) energy per lattice site for a bulk phase as

$$\begin{aligned} \frac{f}{k_B T} = & \rho_A \ln \rho_A + \frac{\rho_B}{N} \ln \rho_B + (1 - \rho_A - \rho_B) \ln(1 - \rho_A - \rho_B) \\ & + \chi_{AC} \rho_A (1 - \rho_A - \rho_B) + \chi \rho_B (1 - \rho_B). \end{aligned} \quad (2.2)$$

For convenience, we switched to reduced densities, i.e.,  $\rho b^3 \mapsto \rho$ , where  $b$  is the size of a lattice site. If we consider a phase-separated system where the volumes of the three phases are large, we can neglect the contribution of the interfaces to the free energy. In that case we may write for the total free energy

$$F = \sum_{j=1}^3 \frac{V^{(j)}}{b^3} f(\rho_A^{(j)}, \rho_B^{(j)}), \quad (2.3)$$

where  $V$  is the volume and the superscript  $(j)$  identifies the phase. To obtain the composition and volumes of the three phases in equilibrium, one has to minimize the total free energy with the boundary conditions that the total volume remains constant, and that the number of molecules of every type is conserved. This optimization can be carried out using a Lagrange method by introducing the following function

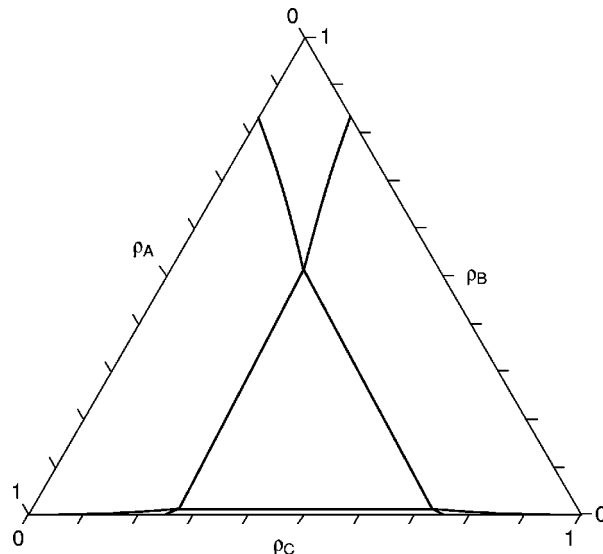


FIG. 3. Ternary phase diagram for a system containing the components  $A$ ,  $B_{10}$ , and  $C$  as calculated with the Flory–Huggins lattice theory. The interaction parameters are chosen such that a three-phase region (the central triangle) exists:  $\chi_{AC} = 2.2$  and  $\chi_{AB} = \chi_{BC} = 1.5$ .

$$\begin{aligned} g = & \sum_{j=1}^3 \frac{V^{(j)}}{b^3} f(\rho_A^{(j)}, \rho_B^{(j)}) - \mu_A \left( \sum_{j=1}^3 \frac{V^j}{b^3} \rho_A^{(j)} - n_A \right) \\ & - \mu_B \left( \sum_{j=1}^3 \frac{V^{(j)}}{b^3} \rho_B^{(j)} - n_B \right) + \Pi \left( \sum_{j=1}^3 V^{(j)} - V \right), \end{aligned} \quad (2.4)$$

where  $n_x$  is the total number of segments of type  $x$ . The chemical potentials of component  $A$  and  $B$  are reflected in the Lagrange parameters  $\mu_A$  and  $\mu_B$ , respectively. The parameter coupled to the constant-volume constraint is the osmotic pressure  $\Pi$ . Minimization can only be carried out numerically. To this end we used a program developed by Linse.<sup>15</sup>

To give an idea about the nature of the ternary phase diagram of the systems under study we calculated the phase-equilibria for the  $A/B_{10}/C$  system. Figure 3 depicts the phase diagram with  $\chi_{AC} = 2.2$  and  $\chi = 1.5$ . The central triangle corresponds to the three-phase region, necessary for wetting. In Fig. 4 the effect of lowering  $\chi$  on the size of the three-phase region is shown. The critical interaction parameter  $\chi_c$ , below which no three-phase region exists, is approximately equal to (but larger than) that in a two-phase system, which is given by

$$\chi_c = \frac{1}{2}(1 + N^{-1/2})^2, \quad (2.5)$$

which is approximately 0.866 for  $N = 10$ . This is indeed in accordance with the numerical calculations visualized in Fig. 4. It should be noted that when the chain length  $N$  is increased the base of the triangle will be much closer to the  $\rho_C$  axis in the phase diagram.

The calculations for the inhomogeneous systems, i.e., where interfacial effects are relevant, are performed using the SF SCF theory. The system containing the flexible polymer is situated on a simple cubic lattice with an *a priori* step probability  $\lambda_1 = 1/6$ . The chain conformations are generated using first-order Markoff statistics. The conformations of the

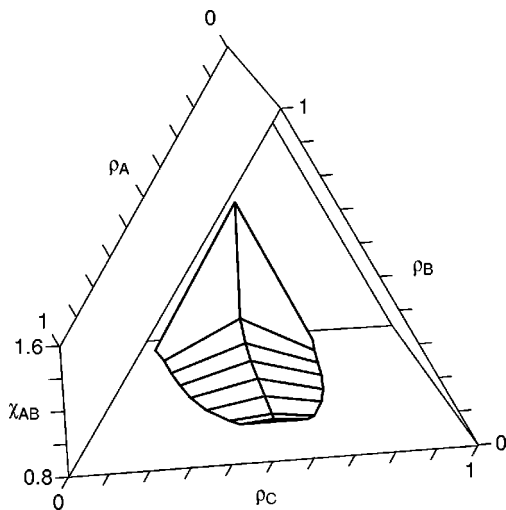


FIG. 4. Change of the three-phase region in the  $A/B_{10}/C$  system as a function of the interaction parameter  $\chi_{AB}$ , with  $\chi_{AC}=2.2$  and  $\chi_{BC}=\chi_{AB}$ .

semiflexible polymer are created by third-order Markoff statistics, i.e., a RIS model is used. This model implies a tetrahedral lattice for the bond correlations. Therefore, we also used a tetrahedral lattice for the interactions. The one-dimensional gradient has its direction perpendicular to the interface, and thus, there is a mean field in two directions parallel to the interface.

In the systems under study here it is most convenient to work in the canonical ( $nVT$ ) ensemble. One should bear in mind that in an SCF model there may exist values of  $\Theta_B^{\text{exc}}$  (or  $\Theta_B$ ) which do not correspond to an equilibrium situation [see Figs. 2(b) and (h)]. This is fully comparable to the so-called Van der Waals loop in liquid–vapor systems. This means that when the number of different molecules in the generated system is fixed, the system will correspond to a point along this loop (or adsorption isotherm).

The systems in this study consist of  $m$  parallel lattice layers, and the number of sites per layer is chosen as  $l=1$ , so the total number of sites, or reduced volume, is  $m$ . The number of layers is chosen large enough, so that no significant finite-size effects occur. The dimensionless excess amount ( $\Theta_x^{\text{exc}}/lb^2 \mapsto \Theta_x^{\text{exc}}$ ) is calculated from the SF SCF solution by

$$\Theta_x^{\text{exc}} = \int_0^{z_G} dz' (\rho_x(z') - \rho_x^{(1)}) + \int_{z_G}^m dz' (\rho_x(z') - \rho_x^{(3)}), \quad (2.6)$$

where  $\rho_x^{(j)}$  denotes the bulk reduced density of component  $x$  in phase  $j$  (see Fig. 1). The reduced distance is defined as  $z' \equiv i - 1/2$ , where  $i$  is the layer number. The Gibbs dividing plane, located at  $z_G$ , is defined by  $\Theta_A^{\text{exc}} = \Theta_C^{\text{exc}}$ . Taking equal amounts of  $A$  and  $C$  ( $\Theta_A = \Theta_C$ ) this choice leads to  $z_G = (m+1)/2$  for the symmetric case studied here. With this in mind we define the reduced distance from the “interface” as  $z \equiv i - z_G$ . Phase separation between the  $A$ - and the  $B$ -rich phase is ensured by setting the Flory–Huggins parameter  $\chi_{AC}=2.2$ , i.e., substantially beyond the critical point. This parameter is held constant throughout this paper.

An important quantity in wetting studies is the excess free energy, i.e., that part of the free energy that can not be

attributed to the bulk phases in the system. This part is a further characteristic of the wetting behavior. As long as no third macroscopic phase is formed, the interfacial tension is simply defined as  $\gamma = F^{\text{exc}}/(b^2l)$ . When a third phase emerges, i.e., when two interfaces exist, the two interfacial tensions are equal in the symmetric system, and hence may be defined by  $\gamma = F^{\text{exc}}/(2b^2l)$ . A final useful quantity in this study is the chemical potential, which in the Flory–Huggins theory and within our restrictions to the system is given by

$$\frac{\mu_B}{k_B T} = \ln \rho_B - N \ln(1 - \rho_A - \rho_B) - N + 1 + \chi(1 - 2\rho_B) + N\chi_{AC}\rho_A, \quad (2.7)$$

for component  $B$ . Because we will be focussing on component  $B$ , we shall further omit this subscript in all molecular properties. For interpreting the wetting phenomena, we need the difference between the chemical potential of a component in a system and that of the same component at the coexistence line, i.e., one is interested in  $\mu - \mu_0$ . This difference is, for component  $B$ , approximated by

$$\mu - \mu_0 = k_B T \ln \frac{\rho}{\rho_0}. \quad (2.8)$$

In this paper we only use dimensionless quantities. To this end we introduce the following rescaling

$$\frac{F^{\text{exc}}}{lk_B T} \mapsto F^{\text{exc}}, \quad \frac{\gamma b^2}{k_B T} \mapsto \gamma, \quad \frac{\Delta u_{\text{tg}}}{k_B T} \mapsto \Delta u_{\text{tg}}, \quad (2.9)$$

$$\frac{\mu}{k_B T} \mapsto \mu, \quad \frac{q}{b} \mapsto q.$$

### III. RESULTS AND DISCUSSION

#### A. Flexible polymer

##### 1. Polymer–solvent interaction

We start with the wetting behavior of a flexible polymer  $B_{100}$  at a liquid–liquid interface as found by the SF SCF theory, using first-order Markoff statistics. An adsorption isotherm is determined by increasing the total amount  $\Theta$  of  $B$ , while keeping the total volume and the  $\Theta_A/\Theta_C$  ratio constant. Instead of the temperature, we use the interaction parameter  $\chi_{AB}$  to scan through the wetting phase diagram. Every point along the isotherm corresponds to an SF SCF solution. This leads to an isotherm which, when in the prewetting or partial-wetting regime, contains a loop as discussed in Sec. II.

Suppose the interaction parameters of a system are such that a prewetting step exists in the adsorption isotherm, i.e., there is a finite jump in the excess amount  $\Theta^{\text{exc}}$  at a certain  $\mu$ . The chemical potential at which this jump occurs can be deduced from the fact that the two different adsorption layers (1 and 2) are subject to the equilibrium conditions:  $\mu^{(1)} = \mu^{(2)}$  and  $\gamma^{(1)} = \gamma^{(2)}$ . This means that plotting the excess free energy as a function of the chemical potential reveals, from the intersection point, the conditions for the finite jump in  $\Theta^{\text{exc}}$ . Such a plot is given in Fig. 5, which will be discussed in detail below. In the case of complete wetting  $F^{\text{exc}}$  is a continuously decreasing function of  $\mu$  up to  $\mu = \mu_0$

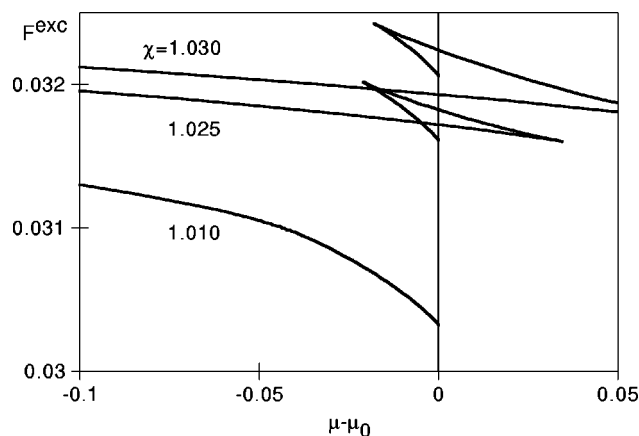


FIG. 5. Excess free energy for the  $A/B_{100}/C$  system where  $B_{100}$  is a flexible polymer. The curves represent the change in  $F^{\text{exc}}$  along three adsorption isotherms with  $\chi_{AC}=2.2$ . From bottom to top we distinguish typical curves for complete wetting ( $\chi=1.01$ ), a system with a prewetting step ( $\chi=1.025$ ), and a case corresponding to partial wetting ( $\chi=1.03$ ).

where the macroscopic phase is formed. The case of partial wetting requires some more explanation. For this system an infinite jump in  $\Theta^{\text{exc}}$  occurs at  $\mu=\mu_0$ , which is equivalent to the formation of an adsorbed layer (1) in equilibrium with a droplet (2). In the symmetric system under study, the equilibrium conditions now read:  $\mu^{(1)}=\mu^{(2)}=\mu_0$  and  $\gamma^{(1)}=2\gamma^{(2)}\cos\theta$ , where  $\gamma^{(1)}=\gamma_{13}$ ,  $\gamma^{(2)}=\gamma_{12}=\gamma_{23}$ , and  $\theta=\theta_1=\theta_3$  (for the symbols see Fig. 1). So, from the excess free energies at  $\mu=\mu_0$  the contact angle can be determined in the following way:

$$\cos\theta = \frac{F_{(1)}^{\text{exc}}}{F_{(2)}^{\text{exc}}}, \quad (3.1)$$

where  $F_{(1)}^{\text{exc}}$  denotes the excess free energy for the system with an adsorbed layer, and  $F_{(2)}^{\text{exc}}$ , that of the system with a macroscopic layer.

With the above in mind it is easy to interpret the  $\mu$ -dependence of the excess free energy as given in Fig. 5 for different values of  $\chi$ . With increasing  $\chi$  we observe three principally different adsorption isotherms: from a complete wetting isotherm ( $\chi=1.01$ ) via an isotherm with a step characteristic for prewetting ( $\chi=1.025$ ) to an isotherm corresponding to partial wetting ( $\chi=1.03$ ). In order to visualize this transition we plot a few typical adsorption isotherms in Fig. 6. The positions of the finite jumps in  $\Theta^{\text{exc}}$  are also indicated, through a pair of filled circles at the same  $\mu$  for each jump. One observes that the magnitude of this jump increases when it occurs closer to  $\mu=\mu_0$  and it diverges at  $\mu=\mu_0$ . This is similar to the observations made in Sec. I.B. for a solid surface. Clearly, the system undergoes a first-order wetting transition. In line with the introduction (Fig. 2), we plot a wetting phase diagram in Fig. 7 based on the calculations from Figs. 5 and 6. In this diagram the horizontal line represents the border line between a one-phase and a two-phase system in a homogeneous bulk. Along this line there will be complete wetting for  $\chi_c < \chi \leq \chi_w$ , where  $\chi_c \approx 0.605$  according to Eq. (2.5) and  $\chi_w \approx 1.0275$  as deduced from the SF SCF computations. Beyond  $\chi_w$ , which we call

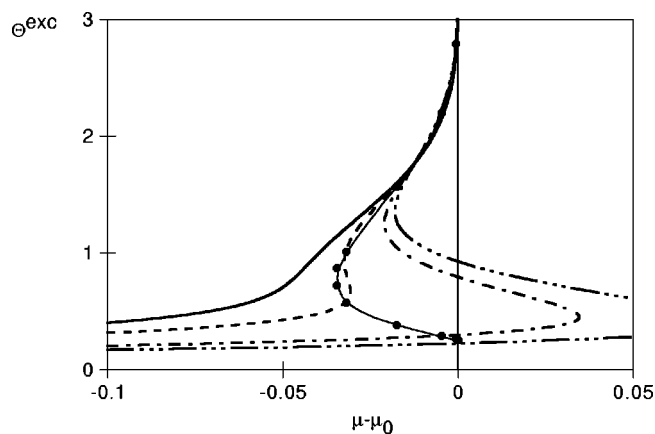


FIG. 6. Adsorption isotherms for the flexible polymer  $B_{100}$  in the  $A/B_{100}/C$  system with  $\chi_{AC}=2.2$ . For the curves from left to right the interaction parameter  $\chi$  is given by 1.01, 1.015, 1.025, and 1.03, respectively (see also Fig. 7). The solid line with the filled circles indicates the prewetting region as determined from the adsorption isotherms (not all shown).

the wetting interaction parameter, partial wetting will occur. The  $\chi$ -interval for which a finite jump in the excess amount occurs in the adsorption isotherm is given by  $\chi_{\text{pw}} < \chi < \chi_w$  where the prewetting critical endpoint in terms of the interaction parameter  $\chi_{\text{pw}}=1.014$  (compare Fig. 6).

One of the quantities that is experimentally accessible in a 3-phase system is the contact angle. This, of course, means that we should be studying a system in the partial-wetting regime. For the system discussed above, this implies that  $\chi > \chi_w$ . The contact angle  $\theta$ , or better  $\cos\theta$ , is calculated with Eq. (3.1) from the SF SCF excess free energies. Figure 8 shows the decrease of  $\cos\theta$  with increasing  $\chi$ . The discontinuity in the derivative of this function at  $\chi \approx 1.0275$  implies that the phase transition is of *first* order. From the figure it can also be seen that a relatively small increase in the interaction between polymer and solvent suffices to cause the polymer-rich droplet to adopt an almost spherical shape. This observation should be no surprise, and can be explained in terms of interfacial tensions. The interfacial tension  $\gamma_{13}$  of an interface with a small amount of polymer deviates only slightly from that of the interface in the binary  $A/C$  system without polymer. However, the interfacial tension  $\gamma_{12}$  between the droplet and the  $A$ -rich phase depends strongly on

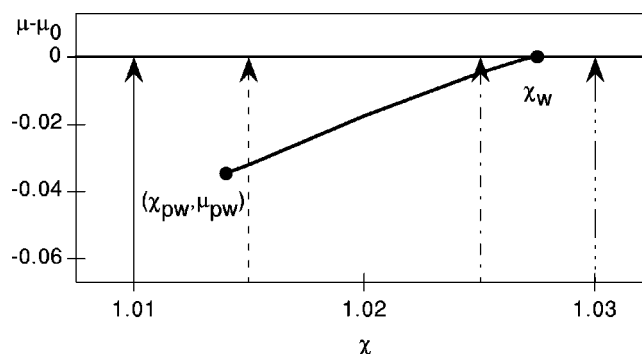


FIG. 7. Wetting phase diagram for the system  $A/B_{100}/C$  with a flexible polymer present and  $\chi_{AC}=2.2$ . The arrows correspond to the adsorption isotherms shown in Fig. 6. For further explanation see Fig. 2 and the text.

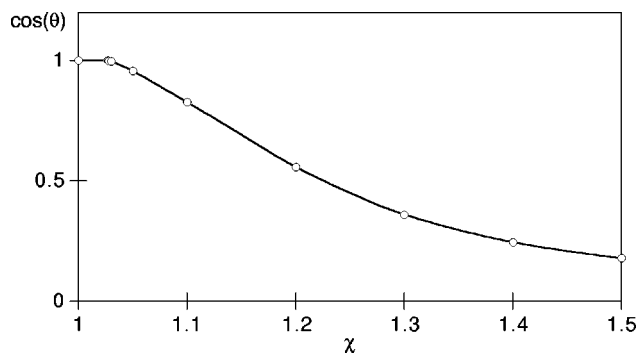


FIG. 8. Contact angle for a  $B_{100}$ -rich phase in equilibrium with an  $A$ - and a  $C$ -rich phase (partial wetting). The discontinuity in  $d \cos \theta / d\chi$  around  $\chi = \chi_w \approx 1.0275$  indicates a first-order phase transition.

the interaction parameter  $\chi$ . This implies that  $\cos \theta$  should indeed decrease rather strongly with increasing  $\chi$ .

## 2. Effect of chain length on the wetting transition

Above we have shown that a simultaneous change of the solubility of a flexible polymer in two monomeric solvents can induce a first-order wetting phase transition. Now we take a closer look at the transition itself. One way to do this is to change the polymer in such a way that the critical interaction parameter  $\chi_c$  changes, by varying the polymer length  $N$  [see Eq. (2.5)]. We computed a number of adsorption isotherms for several values of  $N$  to find the characteristic points in the corresponding wetting phase diagrams:  $(\chi_w, \mu_0)$  and  $(\chi_{pw}, \mu_{pw})$ , see Fig. 7.

The  $N$ -dependence of the prewetting interaction parameter  $\chi_{pw}$  and of the wetting interaction parameter  $\chi_w$  is depicted in Fig. 9. The observed decrease of  $\chi_w$  with increasing  $N$  is similar to that of the critical bulk interaction parameter  $\chi_c$ , given by Eq. (2.5), i.e.,  $\chi_c = \chi_w + \chi^*$ , where  $\chi^*$  is almost independent of  $N$  and is in this case given by  $\chi^* \approx 0.423$ . The fact that  $\chi^*$  is almost independent of  $N$  can be traced to the weak  $N$ -dependence of the entropy loss per polymer segment upon transfer from bulk solution to the interfacial region. The arguments validating this statement are as follows.

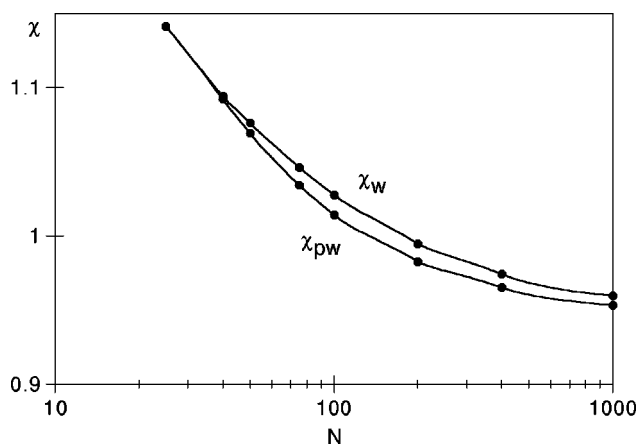


FIG. 9. Wetting interaction parameter  $\chi_w$  and the prewetting critical endpoint in terms of  $\chi_{pw}$  as a function of the chain length  $N$  for the  $A/B_N/C$  system with  $\chi_{AC} = 2.2$ .

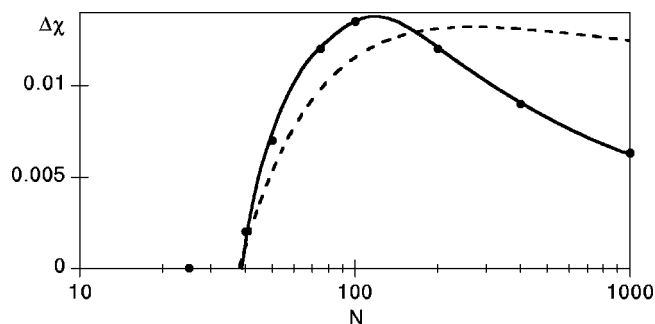


FIG. 10. Location  $\Delta\chi = \chi_w - \chi_{pw}$  of the prewetting critical point in the  $A/B_N/C$  system with  $\chi_{AC} = 2.2$  as a function of chain length. The dotted line indicates an estimate of  $\Delta\chi$  based on a crude thermodynamic model as given by Eq. (3.8). The parameters used are  $\rho^* = 0.061$ ,  $k_p = 0.841$ ,  $d^* = 1.84$ ,  $k_d = 13.25$ , and  $N_c = 38$ .

Within the interfacial region, parts of a polymer chain can freely adopt conformations of typical size  $\xi$ , the width of the interface. If we consider the chain to be subdivided in a number of blobs of size  $\xi$ , then the number of segments in such a blob is given by  $N_\xi \propto \xi^2$ . The entropy loss per ‘‘bond’’ between two blobs can be approximated as  $-\ln(2\lambda_1)$  (which is a positive quantity), so that the entropy loss per polymer segment is about

$$\Delta s \propto -\left(\frac{1}{\xi^2} - \frac{1}{N}\right) \ln(2\lambda_1) \quad \text{for } N > \xi^2. \quad (3.2)$$

Clearly, this entropy loss depends only weakly on  $N$  for the values of  $N$  considered here in the system under study with  $\chi_{AC} = 2.2$ , which corresponds to  $\xi \approx 2.35$ .

A key observation is the fact that the prewetting line vanishes if the chain length approaches  $N \approx 35$  from above. This is easily seen from Fig. 10 where we plot the difference  $\Delta\chi \equiv \chi_w - \chi_{pw}$ , i.e., the difference between the interaction parameter  $\chi$  at the wetting transition and that at the prewetting critical point as a function of chain length. The vanishing prewetting line implies that the wetting transition becomes of second order for  $N \lesssim 35$  under the given circumstances. The change of the order of this wetting transition as a function of  $N$  can be understood in terms of the ratio of the interfacial width of the two-phase system and the coil-size of the polymer. A *first-order* wetting transition is characterized by the fact that a seed is needed to form an additional phase. If the radius of a polymer coil, which is proportional to  $\sqrt{N}$ , is smaller than the interfacial width, the third phase will form continuously without the need for a seed. This situation is referred to as *second-order* wetting.

At this stage it is worthwhile to pay attention to the extension of the prewetting line into the one-phase region, or more precisely to the prewetting critical point. To this end we again refer to Fig. 10, where  $\chi_w - \chi_{pw}$  is plotted as a function of  $N$ . The most remarkable feature of the prewetting critical point is the maximum in  $\Delta\chi(N)$ . The occurrence of such a maximum is far from trivial, and at present we are not able to provide a detailed explanation for this behavior. Instead, we present some thermodynamic considerations which may help to understand why such a maximum could occur.

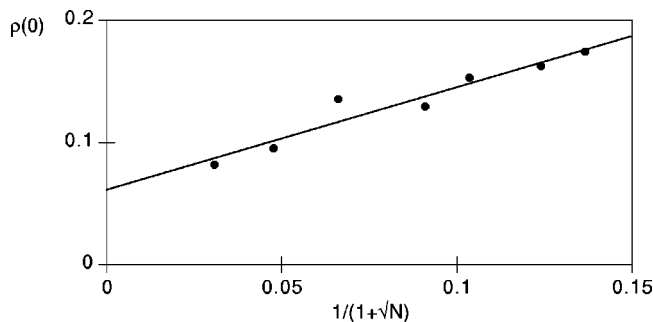


FIG. 11. Reduced density of component *B* at  $z=0$  for the prewetting critical point as a function of  $1/(1+\sqrt{N})$ .

Consider a system for a certain value of  $N$  at its prewetting critical point. In terms of chemical potentials, this point is a distance  $\Delta\mu = \mu_0 - \mu_{pw}$  away from the coexistence line. For  $\mu_0 - \mu < \Delta\mu$  a finite jump in the adsorption isotherm occurs. At the prewetting critical point the extra negative contribution to the interfacial free energy relative to the system at coexistence, at which point a relatively thick layer is formed, is just balanced by the counteracting force to prevent the formation of such a layer before coexistence:

$$\Delta\chi\Delta\rho(1-\Delta\rho) \propto \frac{\Theta^{exc}\Delta\mu}{N}, \quad (3.3)$$

where  $\Delta\mu$  and  $\Delta\chi = \chi_w - \chi_{pw}$  are positive quantities by definition. The reduced density difference,  $\Delta\rho = \rho(0) - \rho(\infty)$ , can be approximated by  $\rho(0)$ , because the bulk reduced density is much smaller than that at the interface. In order to obtain some idea of the  $N$ -dependence of  $\Delta\chi$  we first assume that  $\Theta^{exc} \propto \rho(0)d$ , with  $d$  the width of the density profile of component *B*. Furthermore, we expect that the reduced density at  $z=0$  will follow the critical density  $\rho_c$  for a binary system. We suggest the following empirical relationship:

$$\rho(0) = \rho^* + k_\rho \rho_c, \quad (3.4)$$

where  $k_\rho$  is a constant and  $\rho_c$  is given by

$$\rho_c = \frac{1}{1+\sqrt{N}}. \quad (3.5)$$

The threshold  $\rho^*$  is related to the reduced density at the interface for polymers with infinite chain length, which is necessarily nonzero for wetting. The  $N$ -dependence of  $d$  cannot be principally different from that of  $\rho(0)$ , therefore we assume that

$$d = d^* + \frac{k_d}{1+\sqrt{N}}. \quad (3.6)$$

The numerical results show that Eqs. (3.5) and (3.6) do indeed approximately hold, as can be seen from Figs. 11 and 12, where we plot the reduced density at  $z=0$  and the distance  $d$  from the interface where  $\rho(d) = \rho(0)/2$ . The scatter in these figures is related to the indirect way in which the quantities are determined. The exact position of the prewetting critical point and the quantities derived from it, are extremely sensitive to the exact values of the selected  $\Theta_B$ . Therefore, we can only use the density profiles *near*, and not

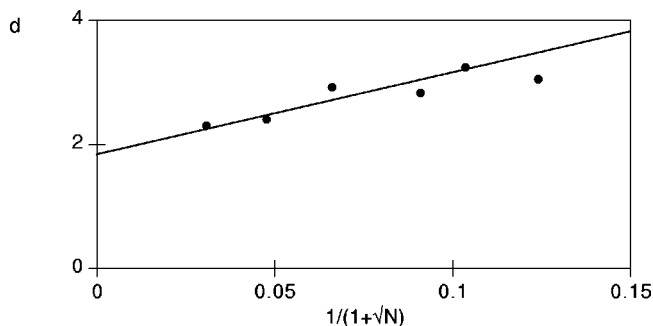


FIG. 12. Width of the density profile at the interface for component *B* at the prewetting critical point as a function of  $1/(1+\sqrt{N})$ .

at, the prewetting critical point. For this reason, it is unsurmountable that one introduces some scatter in the discussed quantities.

Returning to the balance in Eq. (3.3) we finally have to consider the chemical potential difference  $\Delta\mu$ , already introduced above. The contribution of a segment of a polymer chain to the chemical potential difference can reasonably be assumed to be an additive quantity. Note that this can only be the case for first-order wetting, i.e.,  $N > N_c$ . So, we may assume

$$\Delta\mu \propto N - N_c, \quad (3.7)$$

where  $N_c$  is the critical chain length beyond which the wetting transition is of first order under the given circumstances (here  $N_c \approx 35$ ). In Fig. 13 we show the calculated  $\Delta\mu$ , which indicates that Eq. (3.7) is a good approximation. With these rough arguments in mind, we may substitute the above results in Eq. (3.3) and arrive at an approximation for the “width” of the prewetting regime:

$$\Delta\chi \propto \frac{(N - N_c) \left( d^* + \frac{k_d}{1+\sqrt{N}} \right)}{N \left( 1 - \rho^* - \frac{k_\rho}{1+\sqrt{N}} \right)}. \quad (3.8)$$

This expression always gives a maximum for  $\Delta\chi$  as a function of  $N$  for physically feasible values of the introduced constants. An example of this feature is depicted in Fig. 10, where we plot this function, where the values of the different parameters are taken from Figs. 11 and 12,  $N_c = 38$ , and an

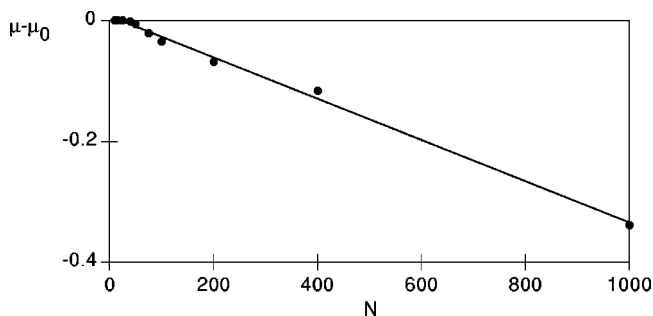


FIG. 13. Chemical potential difference at the prewetting critical point as a function of  $N$ .



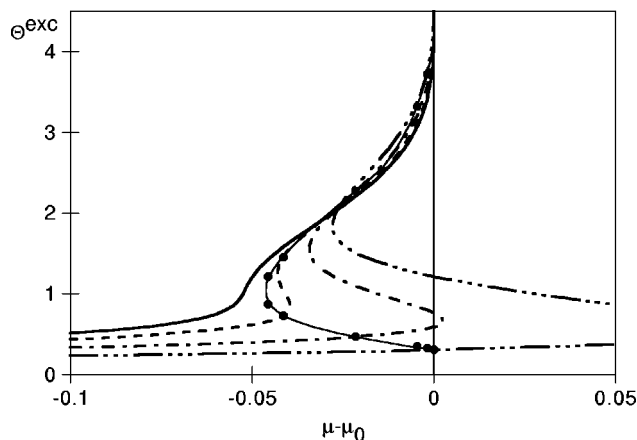


FIG. 14. Adsorption isotherms for the semiflexible polymer in the  $A/B_{100}/C$  system with  $\chi_{AC}=2.2$  and  $\chi=0.94$ . Depicted are the isotherms for  $\Delta u_{tg} = -0.05, 0, 0.1,$  and  $0.25$  (from left to right). The solid line with the filled circles indicates the prewetting region as determined from the adsorption isotherms (not all shown).

arbitrary proportionality constant of  $1/190$  is assumed. Although the function does not entirely fit the data, it is able to describe the main features of  $\Delta\chi$ .

## B. Semi-flexible polymer

In the preceding section we observed that a system with a liquid–liquid interface in the presence of a flexible polymer can undergo a first-order wetting transition if the solubility of the polymer in the two solvents is altered. In a previous paper we studied the adsorption of a semiflexible polymer at a liquid–liquid interface,<sup>1</sup> and concluded that chain stiffness has a noticeable effect on the adsorption behavior. The question arises whether the chain stiffness is also important for the wetting behavior. In other words, is it possible to induce a wetting transition by only changing the chain stiffness? To answer this question we computed a number of adsorption isotherms for a semiflexible polymer  $B_{100}$  with fixed interaction parameters. We chose  $\chi=0.94$  and varied the chain stiffness by taking different values for the energy difference  $\Delta u_{tg}$  between the *gauche* and the *trans* state.

Figure 14 shows the adsorption isotherms for a few values of  $\Delta u_{tg}$ , and Fig. 15 gives the corresponding wetting phase diagram. One may wonder why in Fig. 15 the wetting

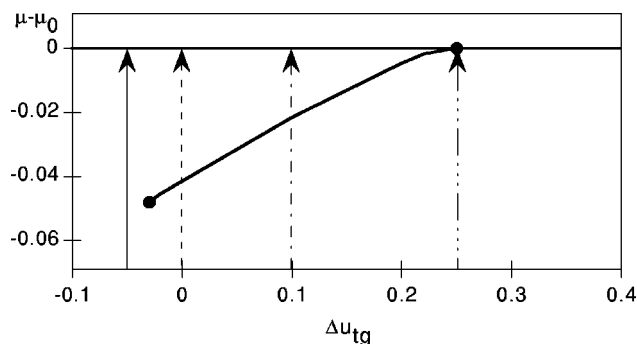


FIG. 15. Wetting phase diagram for the  $A/B_{100}/C$  system in the  $(\Delta u_{tg}, \mu)$  space, with  $\chi_{AC}=2.2$  and  $\chi=0.94$ . The arrows correspond to the isotherms in Fig. 14.

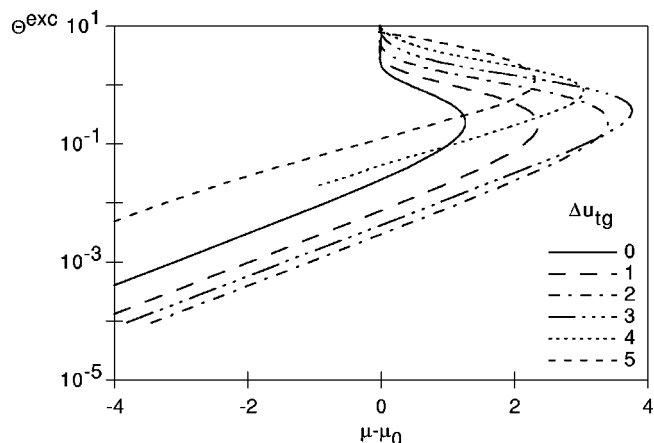


FIG. 16. Adsorption isotherms in the partial-wetting regime for the semiflexible polymer  $B_{100}$  in the  $A/B_{100}/C$  system with  $\chi_{AC}=2.2$  and  $\chi=1.05$ . The energy difference  $\Delta u_{tg}$  is indicated in the figure.

transition occurs at  $\chi \approx 0.94$  for  $\Delta u_{tg}=0$ , whereas in the case of the flexible polymer this transition was found at  $\chi \approx 1.03$ . The difference is caused by the fact that in the RIS scheme  $\Delta u_{tg}=0$  corresponds to  $q=3/2$ , whereas first-order Markoff statistics on a cubic lattice imply  $q=5/4$ . To achieve a persistence length of unity in the RIS scheme one should favor the *gauche* conformation by taking  $\Delta u_{tg} = \ln(5/8) \approx -0.47$ .

Clearly, the question put forward above regarding the chain flexibility can now be answered unambiguously: varying only the chain stiffness is indeed sufficient to induce a wetting transition. The prewetting range, a feature of a first-order transition, is in this case confined to the range  $-0.03 < \Delta u_{tg} < 0.25$  or, equivalently, to  $1.48 < q < 1.69$ . In order to understand this effect of chain stiffness on the wetting behavior of a polymer we return to the key conclusions of our previous paper.<sup>1</sup> The adsorbed amount, at given  $\mu$ , of a semiflexible polymer at a liquid–liquid interface in the dilute regime decreases if  $q/\xi$  is increased up to the point where  $q/\xi \approx 5$ . Here,  $\xi$  represents the dimensionless interfacial width, which can be approximated as  $\xi = \sqrt{2\lambda_1 \chi_{AC} / (\chi_{AC} - 2)}$ . In the system studied here we have  $\xi \approx 2.35$ , which means that one expects the adsorbed amount to decrease for polymers with  $q \leq 11$ , i.e.,  $\Delta u_{tg} \leq 2.7$ . The decrease in adsorbed amount with increasing  $\chi$  is also found for a flexible polymer, in fact for any polymer. This phenomenon is a key effect needed for a wetting transition. We conclude that the predominantly entropic effect which modulates the adsorption behavior of a semiflexible polymer is also responsible for its wetting behavior. However, the question remains as to what happens if we further increase the polymer stiffness.

To answer this question we calculated a number of adsorption isotherms for two values of  $\chi$  (0.94 and 1.05) and values of  $\Delta u_{tg}$  ranging from 0 to 5. The isotherms for  $\chi=1.05$  (completely in the partial-wetting regime) are shown in Fig. 16, now in a logarithmic plot in order to see the effect on the adsorbed amount more clearly. It can be seen that the adsorbed amount in the low  $\Theta^{\text{exc}}$  branch of the isotherm goes through a minimum as a function of  $\Delta u_{tg}$ . On the other

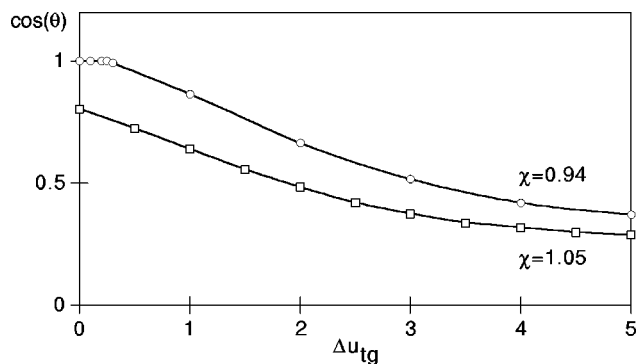


FIG. 17. Contact angle for a  $B_{100}$ -rich phase in equilibrium with an  $A$ - and a  $C$ -rich phase with  $\chi_{AC}=2.2$  and two values of  $\chi$  (as indicated). For  $\chi=0.94$  a first-order phase transition is visible.

hand, the high  $\Theta^{\text{exc}}$  branch does not show such a minimum. On first sight, one could expect that the observed effect on the adsorbed amount should have its impact on the contact angle  $\theta$ . However, as can be seen in Fig. 17,  $\cos \theta$  is a continuously decreasing function of  $\Delta u_{\text{tg}}$  without anomalies. This apparent discrepancy can be understood when one realizes that the effect of the adsorbed polymer on the interfacial tension  $\gamma_{13}$  is small in the low  $\Theta^{\text{exc}}$  branch as compared to the effect achieved by change in stiffness on the interfacial tension  $\gamma_{12}$  between the polymer-rich droplet and the  $A$ -rich phase.

#### IV. CONCLUSIONS

The wetting behavior of both flexible and semiflexible polymers at a liquid-liquid interface has been shown to be extremely rich. With the aid of the SF SCF theory we were able to show that in a symmetric system, i.e.,  $\chi_{AB}=\chi_{BC}=\chi$ , a change in the interaction parameter  $\chi$  induces a wetting transition. For semiflexible polymers it is possible to induce such a transition by solely changing the chain stiffness.

The order of the wetting transition is determined by the

ratio of the interfacial width  $\xi$  of the binary  $A/C$  system and the coil size of the polymer. At fixed  $\xi$  there is a certain chain length  $N_c$  beyond which the wetting transition is of first order, whereas it is of second order for  $N < N_c$ . The features of the prewetting critical point are nontrivial. For the flexible polymer we found that the position ( $\chi_w - \chi_{pw}$ ,  $\mu_0 - \mu_{pw}$ ) of this point has a delicate  $N$ -dependence. We calculated and argued that  $\Delta\chi$  has a maximum as a function of  $N$ . However, further theoretical considerations on this point are desirable.

The approach applied in this paper can be of relevance to wetting systems in polymer blends. The monomeric components used here can easily be replaced by polymeric ones. Also, the nonsymmetric case can be analyzed in detail with our methods. An example of a relevant nonsymmetric system could be the wetting of a liquid-vapor interface by a polymer.

- <sup>1</sup>M. C. P. van Eijk and F. A. M. Leermakers, *J. Chem. Phys.* **109**, 4592 (1998).
- <sup>2</sup>P. G. de Gennes, *Rev. Mod. Phys.* **57**, 827 (1985).
- <sup>3</sup>S. Dietrich, in *Phase Transitions and Critical Phenomena*, edited by C. Domb and J. L. Lebowitz (Academic, London, 1988), Vol. 12, Chap. 1.
- <sup>4</sup>M. Schick, in *Introduction to Wetting Phenomena*, Les Houches, Session XLVIII, 1988—Liquides aux interfaces/Liquids at interfaces, edited by J. Charvolin, J.-F. Joanny, and J. Zinn-Justin (Elsevier, New York, 1990), pp. 415–497.
- <sup>5</sup>A. Yethiraj, S. Kumar, A. Hariharan, and K. S. Schweizer, *J. Chem. Phys.* **100**, 4691 (1994).
- <sup>6</sup>S. K. Kumar, A. Yethiraj, K. S. Schweizer, and F. A. M. Leermakers, *J. Chem. Phys.* **103**, 10332 (1995).
- <sup>7</sup>D. T. Wu, G. H. Fredrickson, and J. P. Carton, *J. Chem. Phys.* **104**, 6387 (1996).
- <sup>8</sup>J. P. Donley and G. H. Fredrickson, *Macromolecules* **27**, 458 (1994).
- <sup>9</sup>D. T. Wu and G. F. Fredrickson, *Macromolecules* **29**, 7919 (1996).
- <sup>10</sup>J. P. Donley, D. T. Wu, and G. H. Fredrickson, *Macromolecules* **30**, 2167 (1997).
- <sup>11</sup>A. Budkowski, J. Rysz, F. Scheffold, and J. Klein, *Europhys. Lett.* **43**, 404 (1998).
- <sup>12</sup>J. M. H. M. Scheutjens and G. J. Fleer, *J. Phys. Chem.* **83**, 1619 (1979).
- <sup>13</sup>J. M. H. M. Scheutjens and G. J. Fleer, *J. Phys. Chem.* **84**, 178 (1980).
- <sup>14</sup>F. A. M. Leermakers and J. M. H. M. Scheutjens, *J. Chem. Phys.* **89**, 3264 (1988).
- <sup>15</sup>P. Linse, POLYMER, Release 2.6.9, Lund University, 1995.